Inventum Biologicum: *An International Journal of Biological Research*
2026, Vol. 6, Issue 3, pp. 41-51

Inventum Biologicum

Journal homepage: www.journals.worldbiologica.com/ib

Research paper

Exploring the Role of Molybdenum Nanoparticles in Catalyzing Nitrate Reductase Activity in Wheat (*Triticum aestivum*): An In Vitro Study

Shweta Alhan [a], **Naresh Tanwer** [b], **Geeta Dhania** [a] *

[a] *Department of Environmental Science, Maharshi Dayanand University, Rohtak, (Haryana), India*
[b] *Central Pollution Control Board, Industrial Pollution Control-I Division, Delhi (Delhi), India*

ARTICLE INFO

Keywords

molybdenum nanoparticles
nitrate reductase
wheat
nitrogen metabolism
nano-fertilizer
in vitro enzyme assay

DOI
10.5281/ib-MSNumber

***Corresponding author**
Geeta Dhania
✉ **Email**
geetadhaniaevs@gmail.com

ABSTRACT

Nitrogen use efficiency (NUE) is a major determinant of crop productivity, yet substantial nitrogen losses during fertilizer application reduce agricultural sustainability and contribute to environmental pollution. Nitrate reductase (NR), a molybdenum-dependent enzyme, catalyses the first and rate-limiting step of nitrate assimilation, making molybdenum availability essential for efficient nitrogen metabolism. The present study aimed to synthesize and characterize molybdenum trioxide (MoO_3) nanoparticles and evaluate their catalytic influence on nitrate reductase activity in wheat (*Triticum aestivum*) under in vitro conditions. MoO_3 nanoparticles were synthesized using a wet chemical route followed by calcination at 500°C and characterized by UV-Visible spectroscopy, zeta potential analysis, Fourier Transform Infrared Spectroscopy (FTIR), Scanning Electron Microscopy (SEM), Energy Dispersive X-ray Spectroscopy (EDS), and X-ray Diffraction (XRD). The synthesized nanoparticles exhibited characteristic optical absorption, moderate colloidal stability (-25 mV), crystalline MoO_3-specific functional groups, high elemental purity, and well-defined crystalline diffraction peaks, confirming successful nanoparticle synthesis. The catalytic effect of Nano-MoO_3 was assessed by measuring nitrate reductase activity at five concentrations (15, 30, 45, 60, and 75 ppm). Enzyme activity increased significantly from 1.21 ± 0.08 to 6.35 ± 0.15 µM NO_2^- g^{-1} h^{-1}, reaching a maximum at 45 ppm, followed by a decline to 3.05 ± 0.10 and 2.48 ± 0.13 µM NO_2^- g^{-1} h^{-1} at 60 and 75 ppm, respectively. Statistical analyses confirmed normality and homogeneity of variance, while one-way ANOVA demonstrated a highly significant effect of Nano-MoO_3 concentration on nitrate reductase activity ($p < 0.001$). Tukey's HSD test identified 45 ppm as the optimum concentration for enzyme activation. These findings demonstrate that appropriately dosed Nano-MoO_3 enhances nitrate reductase activity and possesses considerable potential as a nano-enabled micronutrient for improving nitrogen assimilation and nitrogen use efficiency in wheat.

1. Introduction

Nitrogen (N) is one of the most essential macronutrients required for plant growth, development, and productivity. It is a fundamental constituent of amino acids, proteins, nucleic acids, chlorophyll, enzymes, and numerous metabolites that regulate plant metabolism. Nitrogen availability directly influences photosynthesis, biomass production, grain yield, and crop quality. However, N deficiency remains one of the major factors limiting agricultural productivity worldwide. Although large quantities of nitrogen fertilizers are applied to increase crop yield, only 30-50% of the applied nitrogen is effectively utilized by plants, while the remainder is lost through leaching, runoff, volatilization, and denitrification, resulting in environmental pollution and economic losses (Galloway et al., 2003; Henschke, 2005). Therefore,

improving nitrogen use efficiency (NUE) has become an important objective of sustainable agriculture (Marschner, 1995; Bell & Henschke, 2005; Rahman et al., 2021). Plants absorb nitrogen primarily in two inorganic forms, nitrate (NO_3^-) and ammonium (NH_4^+), from the soil (Imran et al., 2019; Li et al., 2020). Among these, NO_3^- is the predominant nitrogen source for most agricultural crops because of its higher mobility, lower toxicity, and ability to be stored in plant vacuoles. Besides serving as a nutrient, nitrate also functions as an important signaling molecule regulating root development, nutrient transport, gene expression, and adaptation to environmental changes (Liu et al., 2017; Alamri et al., 2021; Alhan et al., 2026). However, NO_3^- cannot be directly incorporated into amino acids and proteins. It must first undergo enzymatic reduction to NH_4^+ before assimilation into organic compounds. The reduction of NO_3^- is initiated by nitrate reductase (NR), a cytosolic enzyme that catalyzes the conversion of NO_3^- to nitrite (NO_2^-). NO_2^- is subsequently reduced to NH_4^+ by nitrite reductase (NiR) within chloroplasts. The resulting NH_4^+ is assimilated through the glutamate synthase/glutamine oxoglutarate aminotransferase (GS/GOGAT) pathway to synthesize amino acids, proteins, nucleic acids, chlorophyll, and other N-containing compounds (Imran et al., 2019; Liu, 2022; Alhan & Dhania, 2024). Since NR catalyzes the first and rate-limiting step of NO_3^- assimilation, its activity largely determines N metabolism, NUE, and overall plant growth. Reduced NR activity has been associated with poor N assimilation, lower photosynthetic efficiency, and decreased crop productivity (Drath et al., 2008; Zhang et al., 2012).

Among the micronutrients involved in N metabolism, molybdenum (Mo) plays a unique and indispensable role. Although required only in trace amounts, Mo forms the active metal center of the molybdenum cofactor (MoCo), which is essential for the catalytic activity of NR and several other oxidoreductase enzymes, including nitrogenase, sulfite oxidase, aldehyde oxidase, and xanthine dehydrogenase (Kaiser et al., 2005; Mendel & Schwarz, 2011). Within NR, Mo acts as the catalytic site where NO_3^- is reduced to NO_2^- through electron transfer from nicotinamide adenine dinucleotide with hydrogen (NADH) via flavin adenine dinucleotide (FAD) and cytochrome b_{557}. Consequently, adequate Mo availability is critical for efficient NO_3^- reduction, chlorophyll synthesis, nitrogen assimilation, and normal plant growth (Tejada-Jiménez et al., 2013). Mo deficiency has become increasingly common in agricultural soils due to intensive cultivation, excessive use of nitrogen and phosphorus fertilizers, low organic matter content, and progressive soil acidification. Under acidic conditions, molybdate availability decreases significantly, resulting in reduced NR activity, NO_3^- accumulation in plant tissues, chlorosis, impaired N metabolism, and lower crop yields (von Uexküll & Mutert, 1995; Wang et al., 2002; Gao et al., 2016; Liu, 2022). Therefore, improving Mo availability represents an effective strategy for enhancing N metabolism and fertilizer use efficiency.

Recent advances in nanotechnology have opened new opportunities for improving nutrient delivery in agriculture. Nanoparticles possess unique physicochemical properties, including nanoscale dimensions, high surface-to-volume ratio, enhanced surface reactivity, superior catalytic efficiency, and improved bioavailability compared with conventional bulk materials. These characteristics enable nanoparticles to interact more effectively with biological molecules and improve nutrient utilization while reducing environmental losses (Dimkpa & Bindraban, 2018; Kah et al., 2018). Mo nanoparticles have gained considerable attention because they combine the nutritional significance of Mo with the catalytic advantages of nanotechnology. Their small particle size and large specific surface area are expected to enhance enzyme-nanoparticle interactions, improve electron transfer efficiency, and increase the catalytic activity of NR. These properties make Mo nanoparticles promising candidates for improving N assimilation and developing efficient nano fertilizers (Zhang *et al*., 2022). However, despite the well-established role of Mo in plant nutrition, studies investigating the direct catalytic influence of Mo nanoparticles on NR activity remain limited, particularly under controlled in vitro conditions.

Wheat (*Triticum aestivum* L.) is one of the most important cereal crops worldwide and serves as a staple food for billions of people. Since wheat production requires substantial N inputs, improving NUE is essential for sustainable agriculture. Understanding the interaction between Mo nanoparticles and NR may provide new opportunities to enhance N metabolism without increasing fertilizer application. Therefore, the present study aimed to synthesize and characterize molybdenum oxide (MoO_3) nanoparticles and investigate their catalytic effect on NR activity in wheat under in vitro conditions. The findings contributed to the development of nanoparticle-based strategies for improving N assimilation and sustainable crop production.

2. Material and Methods

2.1 Synthesis of molybdenum oxide nanoparticles

MoO_3 nanoparticles were synthesized by first preparing an aqueous precursor solution of MoO_3 using distilled water. In parallel, an aqueous oxalic acid solution was prepared in a separate conical flask. The MoO_3 solution was magnetically stirred for 1 h, whereas the oxalic acid solution was stirred for 30

min to achieve complete dissolution and ensure the formation of homogeneous precursor solutions. Subsequently, the oxalic acid solution was added dropwise through a burette into the continuously stirred MoO_3 solution over a period of 3 h, allowing controlled nucleation and homogeneous mixing. The resulting solution was then filtered and the precipitate was washed several times with distilled water to remove residual impurities and unreacted precursors. The purified gelatinous precipitate was dried in a hot-air oven at 100°C for 5 h. Finally, the dried precipitate was calcined in a muffle furnace at 500°C for 2 h to obtain highly crystalline MoO_3 nanoparticles (Fig. 1) (Sangwan et al. 2019).

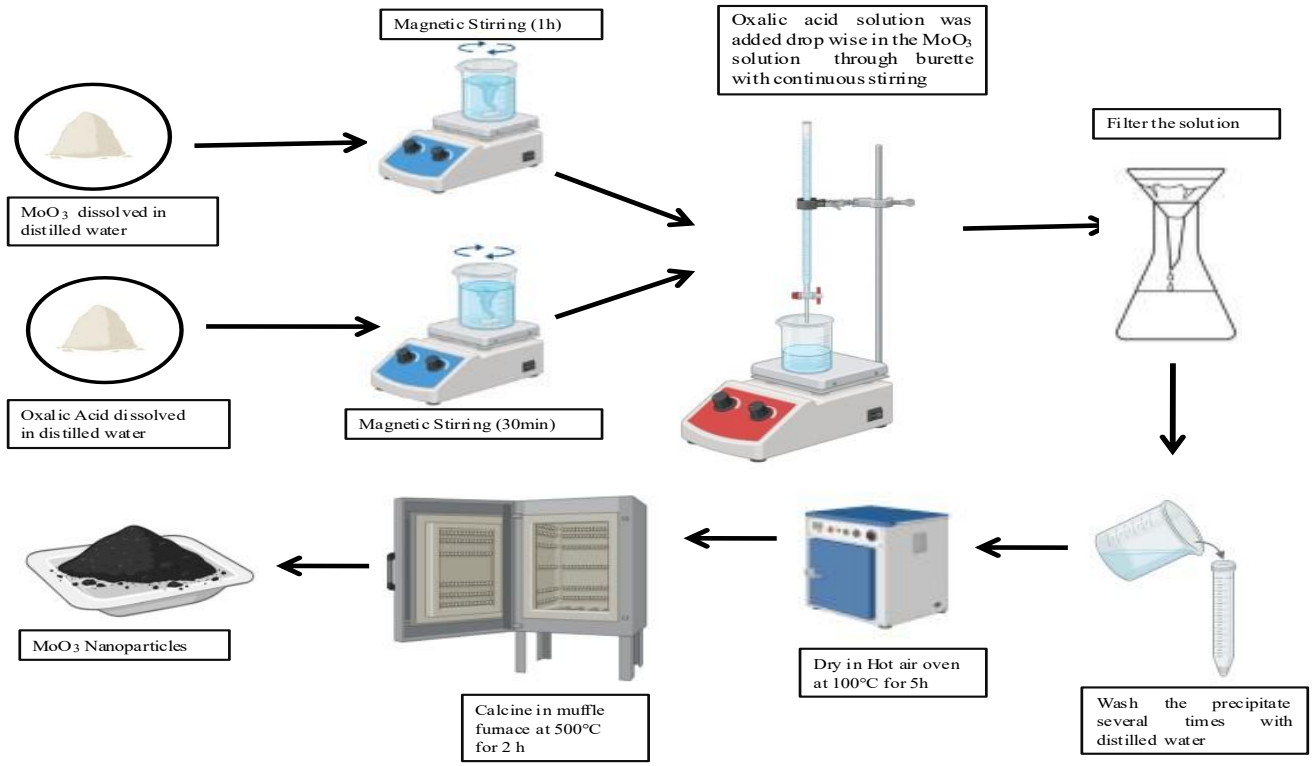

Fig. 1 Systematic representation of synthesis of MoO_3 nanoparticle

2.2 In vitro activity

Wheat (HD-2967) plants were grown in Herbal Garden of Maharshi Dayanand University, Rohtak and nourished with Hoagland solution and harvested at 5-6 leaf stage (1-2 months after plantation) for in vitro activation of enzyme. 0.5g of leaf tissue is washed with distilled water and homogenized in pre cooled mortar pestle by adding 0.1M potassium phosphate, NADH, and 3% Bovine Serum Albumin (BSA) and then crushed and centrifuged at 10,000 rpm for 15 min at 4^0 C. Supernatant was used as crude extract. 1ml of crude leaf extract was used for enzymatic analysis and kept in a water bath for 1 minute at 31^0C. For acid incubation, 0.1 M sodium acetate was utilized with 0.1M of potassium nitrate as substrate, 1ml of Mo nanoparticles (15, 30, 45, 60, and 75 ppm) and Glutathione (GSH) and after that incubated for 30 sec. Again, for neutral incubation, Potassium phosphate was added and incubated at 31^0C for 30 minutes. Then 0.5 ml of 1% sulphanilamide and 0.5ml of 0.05% NNED (Naphthyl ethylene diamine hydrochloride) was added to stop the reaction. After incubation for 15 minutes at 31^0-32^0C, absorbance was taken at 540 nm on UV Spectrophotometer (Ramadoss et al, 1981; Schrader et al, 1974). Then NR Activity was calculated as activity per gram fresh weight (µM NO_2^-. $g^{-1}.h^{-1}$).

$$\text{NR Activity} = \frac{NO_2^-}{T*W}$$

where

$[NO_2^-]$ = conc. of nitrite in µM.
T= Time of incubation(hours).
W= Fresh weight of plant tissue used for extraction(grams)

2.3 Statistical analysis & Quality assurance and quality control

All experimental data were expressed as mean ± standard deviation (SD) of three independent biological replicates (n = 3). Prior to statistical analysis, the normality of the data was evaluated using the Shapiro-Wilk test, while the homogeneity of variances among treatment groups was assessed using Levene's test. Since both assumptions of normality and homogeneity of variance were satisfied ($p > 0.05$), differences in NR activity among Nano-

MoO_3 concentrations were analyzed using one-way analysis of variance (ANOVA), followed by Tukey's Honestly Significant Difference (HSD) test for pairwise comparison of treatment means. Statistical significance was considered at $p < 0.05$. All statistical analyses were performed using IBM SPSS Statistics (IBM Corp., Armonk, NY, USA). Quality assurance and quality control (QA/QC) were maintained by performing all experiments in triplicate (n = 3) under identical experimental conditions. The results are presented as mean ± standard deviation (SD) to ensure the accuracy, precision, and reproducibility of the data.

3. Result and Discussion

The Nano-MoO_3 synthesised in the laboratory was forwarded for various characterizations to depict and verify its physical, chemical and functional properties.

3.1 UV Spectroscopy

UV-Visible spectroscopy of the synthesized MoO_3 nanoparticles showed a strong absorption peak in the 220-240 nm region, confirming the characteristic electronic transitions of MoO_3 (Gedanken, 2005). The absorbance decreased gradually with increasing wavelength, indicating good optical transparency in the visible region. This behaviour confirms the successful formation of crystalline MoO_3 nanoparticles with suitable optical properties for catalytic applications.

3.2 Zeta potential

The zeta potential analysis was carried out to evaluate the surface charge and colloidal stability of the synthesized MoO_3 nanoparticles. The zeta potential distribution exhibited an average zeta potential of -25 mV as shown in Fig. 2, indicating that the nanoparticles possess an overall negative surface charge. This negative surface potential originates from the adsorption of hydroxyl groups and oxygen-containing species on the nanoparticle surface. The observed zeta potential suggests moderate colloidal stability, as nanoparticles with values between ±10 and ±30 mV are generally considered moderately stable in aqueous suspension (Bhattacharjee, 2016). The moderate negative charge reduces excessive particle aggregation through electrostatic repulsion while maintaining sufficient particle interactions, which is consistent with the slight agglomeration observed in the SEM images. Such surface characteristics are beneficial for catalytic applications because they improve nanoparticle dispersion and facilitate interactions with biological molecules. Therefore, the synthesized MoO_3 nanoparticles possess suitable surface stability for in vitro studies.

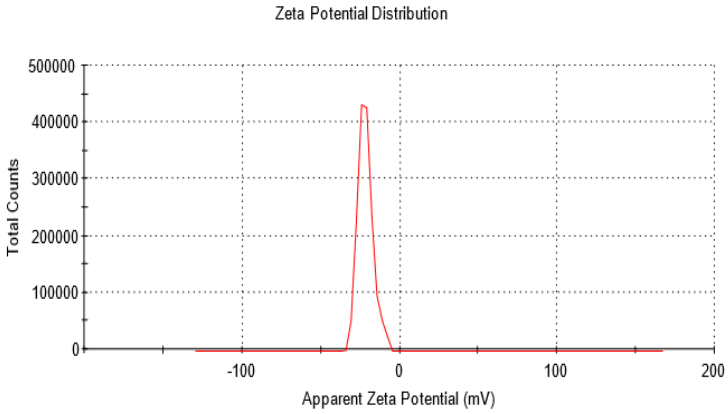

Fig. 2 Zeta potential of synthesized nanoparticles

3.3 Fourier Transform Infrared

Fourier Transform Infrared (FTIR) spectroscopy was employed to identify the functional groups present on the synthesized MoO_3 nanoparticles (as depicted in Fig. 3) and to confirm the formation of the metal oxide phase. A broad absorption band observed in the region of 3455-3214 cm^{-1} was assigned to the stretching vibration of hydroxyl (-OH) groups associated with adsorbed moisture and surface hydroxyl species. These hydroxyl groups enhance the hydrophilicity of nanoparticles and facilitate their interaction with biological molecules (NIST, 2024; Socrates, 2004). The absorption bands at 2929 cm^{-1} and 2867 cm^{-1} correspond to the asymmetric and symmetric stretching vibrations of aliphatic C-H bonds, indicating the presence of trace organic residues from oxalic acid used during synthesis. The peaks observed at 1741 cm^{-1}, 1699 cm^{-1}, and 1649 cm^{-1} were attributed to carbonyl (C=O) stretching vibrations and H-O-H bending of adsorbed water molecules. In addition, the bands at 1543 cm^{-1} and 1515 cm^{-1} are associated with coordinated carboxylate (COO^-) groups, suggesting the transient formation of molybdenum-oxalate complexes during nanoparticle synthesis. The most significant region of the spectrum appears below 1000 cm^{-1}, where characteristic absorption bands are observed at 976, 813, 777, 740, 712, and 681 cm^{-1}. These bands are assigned to terminal Mo=O stretching vibrations, bridging Mo-O-Mo bonds, and O-Mo-O lattice vibrations, which are considered the fingerprint region of crystalline MoO_3 (Malik, et al. 2021). The presence of these characteristic bands confirms the successful formation of crystalline MoO_3 nanoparticles after calcination at 500°C.

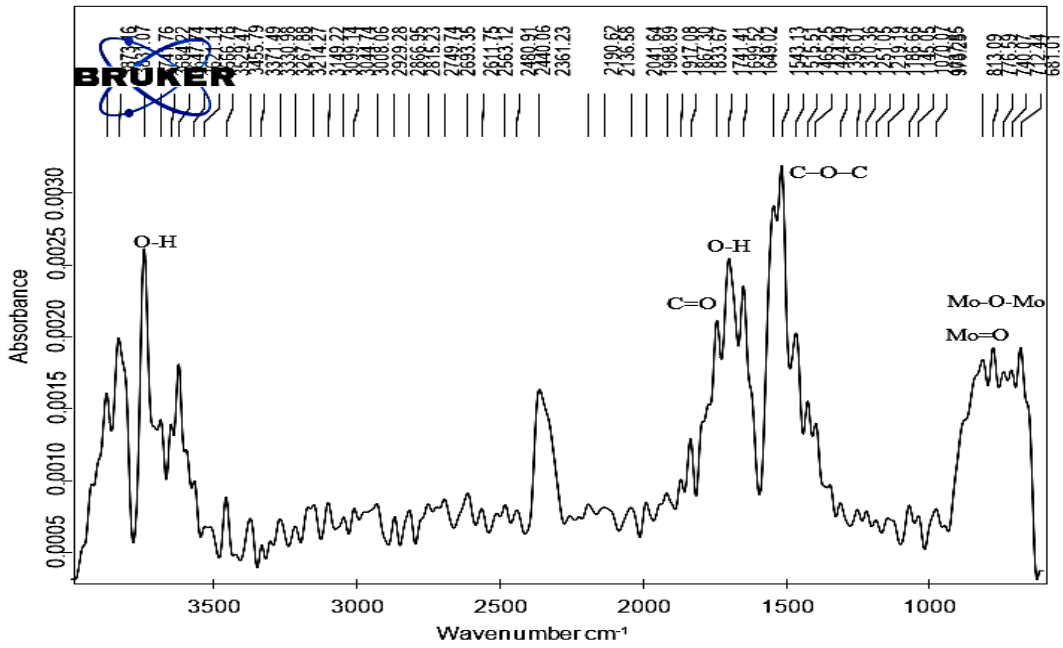

Fig. 3 FTIR spectra of synthesized Mo nanoparticles

3.4 Surface Morphology Analysis

Scanning Electron Microscopy (SEM) analysis was performed at magnifications of 20,000×, and 25,000× to examine the surface morphology of the synthesized MoO_3 nanoparticles. The micrographs revealed predominantly plate-like and irregular polygonal nanostructures with well-defined edges, indicating good crystallinity. Based on the 100 nm scale bar, the individual particles were found to be within the nanometer range (Fig. 4), although some larger aggregates were observed due to particle agglomeration. The aggregation is attributed to the high surface energy and strong interparticle interactions of the nanoparticles. The plate-like morphology provides a relatively high surface area, which is advantageous for catalytic activity. These observations confirm the synthesis of high quality crystalline MoO_3 nanoparticles suitable for catalytic and biological applications.

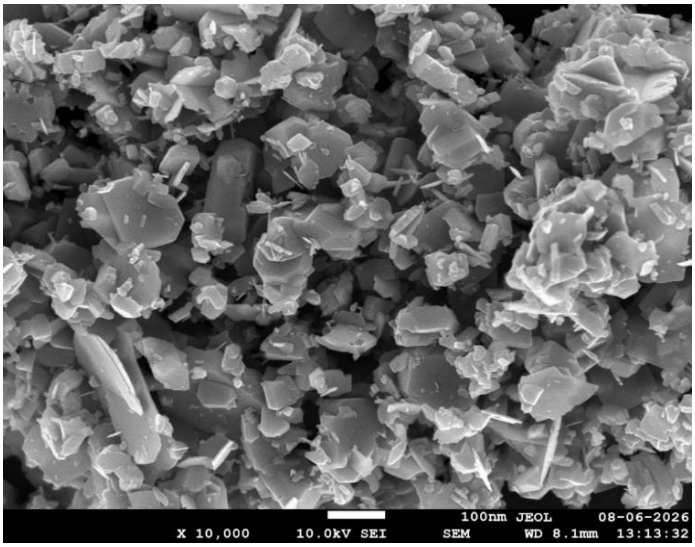

Fig. 4 SEM images of synthesized Nano MoO_3

3.5 EDS Quantitative Analysis

The elemental composition of the synthesized nanoparticles was further evaluated using EDS analysis. The spectra confirmed the presence of Mo as the major constituent along with oxygen and carbon signals. The strong molybdenum peak observed in the EDS spectrum verifies the successful incorporation of molybdenum into the synthesized nanomaterial (Fig 5). Quantitative EDS analysis from different selected regions revealed weight percentages of molybdenum ranging from approximately 16.1% to 38.6%, while oxygen content ranged between 33.7% and 39.1%. Carbon was also detected in varying amounts, likely originating from residual organic compounds, or sample preparation procedures. The substantial oxygen content associated with molybdenum strongly indicates the formation MoO_3-based nanoparticles. The observed elemental ratios suggest that the synthesized material predominantly consists of molybdenum-oxygen frameworks with minor carbonaceous components. The high intensity of molybdenum peaks and the consistent presence of oxygen across different regions confirm the chemical stability and compositional uniformity of the synthesized nanoparticles.

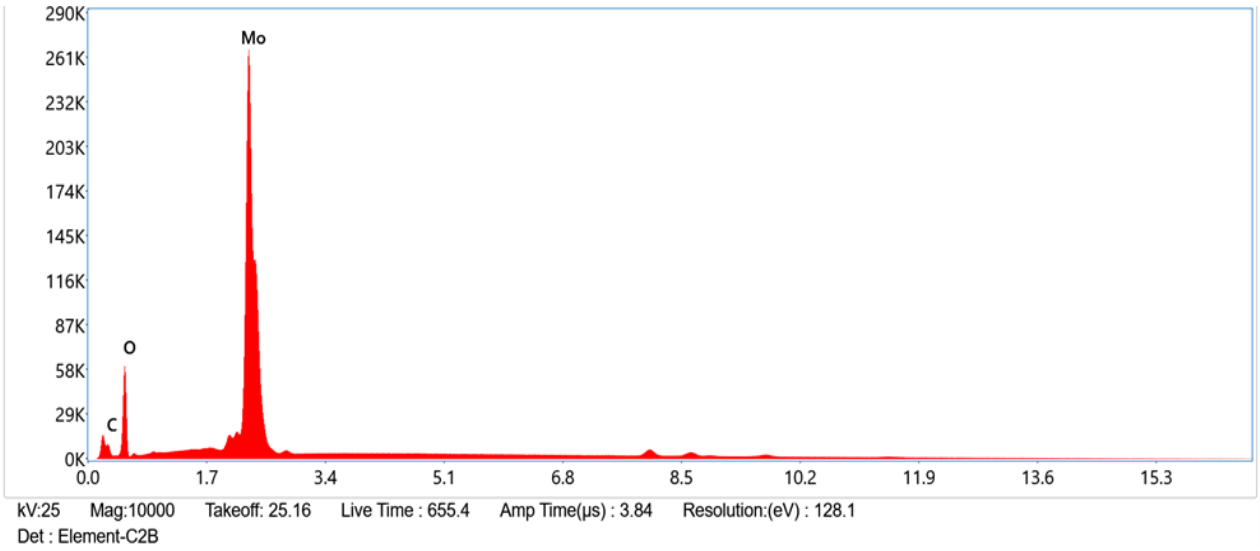

Fig. 5 EDS of synthesized molybdenum nanoparticles

3.6 X-ray diffraction (XRD)

The X-ray diffraction (XRD) pattern was used to investigate the crystalline structure and phase purity of the synthesized MoO_3 nanoparticles. The diffraction pattern exhibited several sharp and well-defined peaks at 2θ values of approximately 27.7°, 32.2°, 38.1°, 44.3°, 46.3°, 54.8°, 64.4°, and 77.4°, confirming the crystalline nature of the synthesized nanoparticles (Fig. 6). These intense diffraction peaks indicate the successful formation of crystalline MoO_3 with high phase purity and negligible amorphous content. The sharpness of the peaks suggests good crystallinity, which was achieved after calcination at 500°C for 2 h.

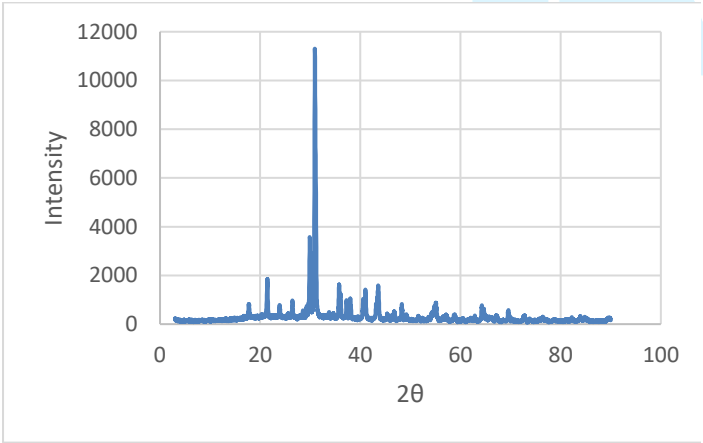

Fig. 6 XRD structure of synthesized nanoparticles

3.7 Nitrate reductase activity

From the literature, it is clear that Mo plays an important role in NR enzymes. These synthesized nanoparticles with varying conditions were used for the activation of NR enzyme. For the proper functioning or to increase the lifetime of nitrate reductase enzyme 3% BSA was used as proteolytic enzyme degrades the enzyme which can lead to degradation of NR. So, BSA was given as food to proteolytic enzymes to protect the NR from degradation. FAD added to give a stabilizing effect to the enzymes. For the activation of enzymes, optimum pH and time is very important. As in vitro enzymatic activity, acidic incubation is necessary for the denaturation of enzymes. This denaturation of enzymes allowed its strands to open and insertion of nano MoO_3 into the enzyme. After Acid Incubation, Neutral incubation was performed to again refolding of the NR enzyme. Also, the time required for acid incubation (unfolding) was the 30s only, and for neutral incubation it was 30min. Formation of NO_2^- is calculated which determined the enzymatic assay of NR. NR activity was calculated as per gram fresh weight (µM NO_2^-. $g^{-1}.h^{-1}$) is given in Table 1.

Table 1 NR enzymatic activity (in µM NO_2^-. $g^{-1}.h^{-1}$) along with nano-molybdenum conc.

Nano-MoO_3 Conc. (ppm)	NR Activity (R1)	NR Activity (R2)	NR Activity (R3)	Mean ± SD
15	1.18	1.30	1.16	1.21 ± 0.08
30	2.74	2.54	2.81	2.70 ± 0.14
45	6.41	6.18	6.46	6.35 ± 0.15
60	2.95	3.14	3.06	3.05 ± 0.10
75	2.36	2.61	2.48	2.48 ± 0.13

Results showed the clear concentration dependent response of enzymatic activity of NR as shown in Table 1. At lowest conc. of Mo nanoparticles enzymatic was found lowest and gradually increased upto maximum activity at 45 ppm concentration of Nano-MoO_3 that is 6.35 ± 0.15 µM NO_2^-. $g^{-1}.h^{-1}$. This demonstrated that 45 ppm Nano-MoO_3 as the optimum concentration for maximum activation of NR enzyme. However, further increase in nanoparticle concentration resulted in a decline in enzyme activity, observed at 60 and 75 ppm, respectively. This reduction suggests that excessive Nano-MoO_3 concentration may negatively influence enzyme activity due to possible nanoparticle-induced stress or disturbance in enzyme

conformation. Tripathi et al, (2017) reported in their studies, where optimal Mo supplementation enhanced nitrate reductase activity, whereas excessive Mo application resulted in reduced enzyme activity and impaired plant physiological performance due to micronutrient imbalance and toxicity.

3.8 Statistical Analysis

The effect of Nano-MoO_3 on NR activity was statistically evaluated using IBM SPSS software. Prior to hypothesis testing, the normality of the data for each treatment group was examined using the Shapiro-Wilk normality test, which is recommended for small sample sizes ($n < 50$) because of its superior statistical power compared with other normality tests (Razali & Wah, 2011; Shapiro & Wilk, 1965). Homogeneity of variances among treatments was assessed using Levene's test, which evaluates whether the variance is equal across treatment groups (Levene, 1960).

Since the assumptions of normality and homogeneity of variance were satisfied ($p > 0.05$), differences in nitrate reductase activity among Nano-MoO_3 concentrations were analyzed using one-way analysis of variance (ANOVA). One-way ANOVA is the most appropriate statistical method for comparing the means of more than two independent treatment groups when parametric assumptions are met (Field, 2018; Montgomery, 2020).

Following a significant ANOVA result, Tukey's Honestly Significant Difference (HSD) post hoc test was performed to identify pairwise differences among treatment means while controlling the family-wise error rate (Tukey, 1949). Statistical significance was considered at $p < 0.05$. Experimental data are presented as mean ± standard deviation (SD) of three independent biological replicates.

3.8.1 Statistical Results

Nano-MoO_3 supplementation produced a significant concentration-dependent effect on NR activity. The enzyme activity increased progressively from 1.21 ± 0.08 µM NO_2^- g^{-1} h^{-1} at 15 ppm to 2.70 ± 0.14 µM NO_2^- g^{-1} h^{-1} at 30 ppm and reached the highest value (6.35 ± 0.15 µM NO_2^- g^{-1} h^{-1}) at 45 ppm. Thereafter, NR activity declined markedly to 3.05 ± 0.10 µM NO_2^- g^{-1} h^{-1} at 60 ppm and further to 2.48 ± 0.13 µM NO_2^- g^{-1} h^{-1} at 75 ppm, demonstrating an optimum Nano-MoO_3 concentration of 45 ppm for enzyme activation.
The Shapiro-Wilk test confirmed that the data for all treatment groups followed a normal distribution ($p > 0.05$) (Table 2), whereas Levene's test indicated homogeneity of variances among treatments ($p > 0.05$) (Table 3). Therefore, one-way ANOVA was performed to compare NR activity among Nano-MoO_3 concentrations.

Table 2 Shapiro-Wilk normality test for NR activity

Nano-MoO_3 concentration (ppm)	W statistic	p-value	Interpretation
15	0.855	0.253	Normal
30	0.928	0.482	Normal
45	0.879	0.321	Normal
60	0.992	0.826	Normal
75	0.999	0.956	Normal

**Significant at $p < 0.05$*

Table 3 Levene's Test for Homogeneity of Variance

Test	Statistic	df1	df2	p-value	Interpretation
Levene's test	0.157	4	10	0.955	Equal variances assumed

One-way ANOVA indicated that Nano-MoO_3 concentration had a highly significant effect on NR activity ($F(4,10) = 758.819$, $p < 0.001$) (Table 4), indicating that enzyme activity differed significantly among the five treatments.

Table 4 One-way ANOVA for the effect of Nano-MoO_3 on NR activity

Source of Variation	Sum of Squares (SS)	df	Mean Square (MS)	F-value	p-value
Between Groups	43.951	4	10.988	758.819	< 0.001
Within Groups (Error)	0.145	10	0.0145		
Total	44.096	14			

Tukey's HSD multiple comparison test further demonstrated that the 45 ppm treatment exhibited significantly greater nitrate reductase activity than all other Nano-MoO_3 concentrations ($p < 0.05$) (Table 5).

Table 5 Tukey's HSD Multiple Comparison Test

Comparison	Mean Difference	Adjusted p-value	Significant
15 vs 30	1.483	<0.001	Yes
15 vs 45	5.137	<0.001	Yes
15 vs 60	1.837	<0.001	Yes
15 vs 75	1.270	<0.001	Yes
30 vs 45	3.653	<0.001	Yes
30 vs 60	0.353	0.031	Yes
30 vs 75	-0.213	0.265	No
45 vs 60	-3.300	<0.001	Yes
45 vs 75	-3.867	<0.001	Yes
60 vs 75	-0.567	0.001	Yes

**Significant at $p < 0.05$*

3.8.2 Statistical Discussion

The present investigation demonstrated a distinct concentration-dependent response of NR activity following Nano-MoO_3 supplementation. The enzyme activity increased progressively from 1.21 ± 0.08 µM NO_2^- g^{-1} h^{-1} at 15 ppm to 2.70 ± 0.14 µM NO_2^- g^{-1} h^{-1} at 30 ppm and reached a maximum of 6.35 ± 0.15 µM NO_2^- g^{-1} h^{-1} at 45 ppm. Beyond this optimum concentration, NR activity decreased significantly to 3.05 ± 0.10 µM NO_2^- g^{-1} h^{-1} at 60 ppm and further to 2.48 ± 0.13 µM NO_2^- g^{-1} h^{-1} at 75 ppm. This bell-

shaped response clearly indicates that moderate concentrations of Nano-MoO_3 effectively enhance nitrate reductase activity, whereas excessive nanoparticle concentrations exert an inhibitory effect on N metabolism.

Prior to hypothesis testing, the assumptions of parametric analysis were evaluated. The Shapiro-Wilk test indicated that the nitrate reductase data for each treatment group were normally distributed ($p > 0.05$), while Levene's test confirmed homogeneity of variances among treatments ($p > 0.05$). Since both assumptions of normality and homoscedasticity were satisfied, one-way analysis of variance (ANOVA) was considered appropriate for comparing treatment means (Field, 2018; Montgomery, 2020). The ANOVA revealed a highly significant effect of Nano-MoO_3 concentration on NR activity ($F(4,10) = 758.82$, $p < 0.001$), demonstrating that the observed differences among treatment means were not attributable to random experimental variation but were primarily caused by Nano-MoO_3 application.

To identify which treatment concentrations differed significantly, Tukey's Honestly Significant Difference (HSD) test was performed following the significant ANOVA result. The post hoc analysis demonstrated that the 45ppm treatment exhibited significantly greater nitrate reductase activity than all other Nano-MoO_3 concentrations ($p < 0.05$), confirming that 45 ppm represented the optimum Nano-MoO_3 concentration for stimulating NR activity under the present experimental conditions. From a physiological perspective, the enhanced NR activity observed at 45 ppm may be attributed to improved Mo availability for the biosynthesis of the Moco, which forms the catalytic centre of NR (Gupta & Lipsett, 1981; Mendel & Bittner, 2006). Adequate Mo availability enhances electron transfer during NO_3^- reduction, thereby increasing NO_3^- assimilation and improving N metabolism. However, excessive Nano-MoO_3 concentrations (60 and 75 ppm) may induce oxidative stress, alter cellular redox homeostasis, interfere with nutrient uptake, or affect enzyme conformation, ultimately reducing catalytic efficiency despite the continued presence of Mo (Rico et al., 2011; Tripathi et al., 2017).

The pairwise comparisons revealed that NR activity increased significantly from 15 ppm to 30 ppm (mean difference = 1.483, $p < 0.001$), indicating that increasing Nano-MoO_3 concentration within the lower dose range substantially enhanced enzyme activity. A much larger and highly significant increase was observed between 15 ppm and 45 ppm (mean difference = 5.137, $p < 0.001$), confirming that 45 ppm produced the greatest stimulatory effect on NR activity. Similarly, significant differences between 15 ppm and 60 ppm (mean difference = 1.837, $p < 0.001$) and between 15 ppm and 75 ppm (mean difference = 1.270, $p < 0.001$) demonstrate that even the higher Nano-MoO_3 concentrations maintained greater enzyme activity than the lowest concentration tested, although their activities were substantially lower than that observed at the optimum concentration.

Comparison of the intermediate concentrations further supported the concentration-dependent response. NR activity at 45 ppm was significantly greater than that at 30 ppm (mean difference = 3.653, $p < 0.001$), demonstrating that increasing Nano-MoO_3 concentration from 30 to 45 ppm resulted in a marked enhancement of enzymatic activity. Likewise, 45 ppm differed significantly from both 60 ppm (mean difference = -3.300, $p < 0.001$) and 75 ppm (mean difference = -3.867, $p < 0.001$), confirming that enzyme activity declined significantly when Nano-MoO_3 concentration exceeded the optimum level. These findings clearly indicate that 45 ppm represents the optimum Nano-MoO_3 concentration for maximizing NR activity under the present experimental conditions.

Interestingly, although NR activity decreased after the optimum concentration, the decline was not uniform across all higher treatments. The comparison between 30 ppm and 60 ppm also showed a statistically significant difference (mean difference = 0.353, $p = 0.031$), indicating that the reduction observed at 60 ppm was sufficient to produce a measurable difference relative to the 30 ppm treatment. In contrast, no significant difference was observed between 30 ppm and 75 ppm (mean difference = -0.213, $p = 0.265$). This result suggests that the nitrate reductase activity recorded at 75 ppm was statistically comparable with that observed at 30 ppm despite their numerical differences. The absence of a significant difference between these two treatments indicates that enzyme activity had declined to a level similar to that produced by the lower Nano-MoO_3 concentration.

Furthermore, 60 ppm and 75 ppm differed significantly (mean difference = -0.567, $p = 0.001$), indicating that the inhibitory effect of Nano-MoO_3 continued beyond 60 ppm. This statistically significant difference demonstrates that nitrate reductase activity did not stabilize after reaching the supra-optimal concentration but instead underwent a further decline as Nano-MoO_3 concentration increased from 60 to 75 ppm. Therefore, the present results suggest a progressive inhibitory effect of excessive Nano-MoO_3 on NR activity rather than the establishment of a stable inhibition plateau. Although Mo is an essential micronutrient, excessive nanoparticle concentrations may disturb cellular homeostasis through increased production of reactive oxygen species (ROS), oxidative damage to proteins and membranes, interference with nutrient uptake, and disruption of intracellular redox balance (Rico et al., 2011; Tripathi et al., 2017).

In nutshell, the Tukey's HSD multiple comparison analysis provides strong statistical evidence that Nano-MoO_3 concentration significantly regulates NR activity in wheat. The results clearly establish 45 ppm as the optimum concentration for enhancing NR activity, while concentrations above this level produce a significant decline in enzyme activity. These findings emphasize that precise optimization of Nano-MoO_3 dosage is essential to maximize nitrogen assimilation and improve nitrogen use efficiency while avoiding the adverse physiological effects associated with excessive nanoparticle exposure. Similar improvements in NR activity and N metabolism following Mo supplementation have been reported in wheat and several other crop species (Imran et al., 2015; Sangwan et al., 2019).

Overall, the statistical analysis strongly supports the biological observations obtained in the present study. The combination of normally distributed data, homogeneous variances, highly significant one-way ANOVA results, and Tukey's HSD multiple comparisons provides robust evidence that Nano-MoO_3 concentration significantly regulates NR activity in wheat. Among the tested concentrations, 45 ppm was identified as the optimum dose, producing the highest NR activity and demonstrating the greatest potential to improve NO_3^- assimilation and NUE. These findings highlight the importance of optimizing nanoparticle dosage, as appropriate Nano-MoO_3 supplementation can enhance N metabolism, whereas excessive concentrations may adversely affect plant physiological processes.

4. Conclusion

The present study successfully synthesized crystalline MoO_3 nanoparticles using a simple wet chemical method followed by calcination. Comprehensive characterization by UV-Visible spectroscopy, zeta potential analysis, FTIR, SEM, EDS, and XRD confirmed the successful formation of moderately stable, crystalline MoO_3 nanoparticles with physicochemical properties suitable for biological applications. The in vitro enzyme assay demonstrated that Nano-MoO_3 significantly influenced NR activity in a concentration-dependent manner. Among the tested concentrations, 45 ppm produced the highest NR activity (6.35 ± 0.15 µM NO_2^- g^{-1} h^{-1}), indicating that this concentration provides optimum Mo availability for activation of the Moco and efficient NO_3^- reduction. In contrast, higher concentrations (60 and 75 ppm) reduced enzyme activity, suggesting that excessive Nano-MoO_3 may impair NO_3^- metabolism through nanoparticle-induced physiological stress or disruption of cellular homeostasis.

Statistical analyses, including the Shapiro-Wilk test, Levene's test, one-way ANOVA, and Tukey's HSD multiple comparison test, confirmed that the observed differences among treatments were statistically significant and identified 45 ppm as the optimum Nano-MoO_3 concentration for enhancing NR activity. These results demonstrate that carefully optimized Nano-MoO_3 supplementation can substantially improve NO_3^- assimilation, thereby providing a promising strategy for enhancing NUE.

Although the present investigation was conducted under in vitro conditions, the findings establish a strong mechanistic basis for the use of Nano-MoO_3 as a potential nano-fertilizer. Future studies should evaluate its performance under greenhouse and field conditions, investigate its effects on plant growth, nutrient uptake, grain yield, and nitrogen use efficiency, and assess its long-term environmental safety before large-scale agricultural application.

Acknowledgements

The first author acknowledges and thanks to Ministry of Social Justice and Empowerment and the University Grants Commission (UGC) for providing fellowship.

Funding Information

This research did not receive any specific grant from funding agencies in the public, commercial, or not-for-profit sectors.

Declaration of Conflict

The authors declare that they have no known competing financial interests or personal relationships that could have appeared to influence the work reported in this paper.

References

1. Alamri, S., et al. (2021). Nitrogen metabolism and nitrate assimilation in plants. *Plants, 10*, 1-20.
2. Alhan, S., & Dhania, G. (2024). Enhanced nitrogen use efficiency in plants by the application of molybdenum. In Integrating Science and technology: A comprehensive approach to innovation. Notion Press.
3. Alhan, S., Tanwer, N., Dhania, G., 2026. Mitigating nitrogen pollution through molybdenum supplementation: a review on enhancing nitrogen use efficiency in crops. Pollution, 12(1), 462-476 https://doi.org/10.22059/poll.2025.404120.3151
4. Bell, R. W., & Henschke, P. H. (2005). Nutrient management for sustainable agriculture. *Plant and Soil, 274*, 1-12.
5. Bhattacharjee, S. (2016). DLS and zeta potential-What they are and what they are not. *Journal of Controlled Release, 235*, 337-351. https://doi.org/10.1016/j.jconrel.2016.06.017
6. C.S. Ramadoss, T.C. Shen, B. Vennesland (1981), Molybdenum insertion in vitro in demolybdo nitrate reductase of Chlorella vulgaris. *Journal of Biological Chemistry*, 256, 22, 11532-11537. https://doi.org/10.1016/S0021-9258(19)68433-4.

7. Dimkpa, C. O., & Bindraban, P. S. (2018). Nanofertilizers: New products for the industry? *Journal of Agricultural and Food Chemistry, 66*, 6462-6473.
8. Drath, M., et al. (2008). Nitrogen source-dependent regulation of nitrate assimilation in plants. *Plant Biology, 10*, 1-9.
9. Dunn, O. J. (1964). Multiple comparisons using rank sums. *Technometrics, 6*(3), 241-252. https://doi.org/10.1080/00401706.1964.10490181
10. Field, A. (2018). *Discovering statistics using IBM SPSS Statistics* (5th ed.). Sage Publications.
11. Galloway, J. N., Aber, J. D., Erisman, J. W., Seitzinger, S. P., Howarth, R. W., Cowling, E. B., & Cosby, B. J. (2003). The nitrogen cascade. *BioScience, 53*(4), 341–356. https://doi.org/10.1641/0006-3568(2003)053[0341:TNC]2.0.CO;2
12. Gao, S., et al. (2016). Soil acidification and molybdenum availability in agricultural ecosystems. *Soil Science, 181*, 1-10.
13. Gedanken, A. (2004). Using sonochemistry for the fabrication of nanomaterials. *Ultrasonics Sonochemistry, 11*(2), 47-55. https://doi.org/10.1016/j.ultsonch.2004.01.037
14. Gupta, U. C., & Lipsett, J. (1981). Molybdenum in soils, plants, and animals. *Advances in Agronomy, 34*, 73-115. https://doi.org/10.1016/S0065-2113(08)60885-8
15. Imran, M., et al. (2015). Role of molybdenum in improving nitrogen metabolism and crop productivity. *Journal of Plant Nutrition, 38*(13), 2025-2042.
16. Imran, M., Sun, X., Hussain, S., Ali, U., Rana, M. S., Rasul, F., Saleem, M. H., Moussa, M. G., Bhantana, P., Afzal, J., Elyamine, A. M., & Hu, C. X. (2019). Molybdenum-induced effects on nitrogen metabolism enzymes and elemental profile of winter wheat (Triticum aestivum L.) under different nitrogen sources. *International Journal of Molecular Sciences*, *20*(12). https://doi.org/10.3390/ijms20123009
17. Kah, M., et al. (2018). Nanopesticides and nanofertilizers: Emerging contaminants or opportunities? *Nature Nanotechnology, 13*, 677-684.
18. Kaiser, W. M., et al. (2005). Nitrate reductase: Physiology and regulation. *Journal of Experimental Botany, 56*, 875-885.
19. Kruskal, W. H., & Wallis, W. A. (1952). Use of ranks in one-criterion variance analysis. *Journal of the American Statistical Association, 47*(260), 583-621. https://doi.org/10.1080/01621459.1952.10483441
20. Levene, H. (1960). Robust tests for equality of variances. In I. Olkin (Ed.), *Contributions to probability and statistics* (pp. 278-292). Stanford University Press.
21. Li, B., et al. (2013). Effects of nitrate and ammonium nutrition on plant growth and nitrogen metabolism. *Plant Physiology and Biochemistry, 70*, 16-24.
22. Li, B., et al. (2020). Nitrogen uptake and assimilation in higher plants. *Frontiers in Plant Science, 11*, 1-15. https://doi.org/10.3389/fpls.2020.583260
23. Linstrom, P. J., & Mallard, W. G. (Eds.). (2024). *NIST Chemistry WebBook* (NIST Standard Reference Database No. 69). National Institute of Standards and Technology.
24. Liu, X. (2022). Molybdenum regulates nitrate reductase activity and nitrogen metabolism in plants. *Critical Reviews in Plant Sciences, 41*, 1-25.
25. Liu, X., Niu, Y., et al. (2017). Nitrate as a signaling molecule in plants. *Plant Signaling & Behavior, 12*, e1365215.
26. Malik, R., Joshi, N., & Tomer, V. K. (2021). Advances in the designs and mechanisms of MoO_3 nanostructures for gas sensors: A holistic review. *Materials Advances, 2*(13), 4190-4227. https://doi.org/10.1039/D1MA00374G
27. Marschner, H. (1995). *Mineral nutrition of higher plants* (2nd ed.). Academic Press.
28. Marschner, P. (2012). *Marschner's mineral nutrition of higher plants* (3rd ed.). Academic Press.
29. Mendel, R. R., & Bittner, F. (2006). Cell biology of molybdenum. *Biochimica et Biophysica Acta (BBA) - Molecular Cell Research, 1763*(7), 621-635. https://doi.org/10.1016/j.bbamcr.2006.03.013
30. Mendel, R. R., & Schwarz, G. (2011). Molybdenum cofactor biosynthesis in plants. *Annual Review of Plant Biology, 62*, 181-204.
31. Montgomery, D. C. (2020). *Design and analysis of experiments* (10th ed.). John Wiley & Sons.
32. Poonam Sangwan, et al. (2019). Wet chemical synthesis, characterization, and antibacterial activity of molybdenum oxide nanoparticles against *Staphylococcus epidermidis* and *Enterobacter aerogenes*. *Asian Journal of Pharmaceutical and Clinical Research, 12*(4), 59-63. https://doi.org/10.22159/ajpcr.2019.v12i4.30644
33. Rahman, M., et al. (2021). Nitrogen use efficiency in cereal crops: Current status and future prospects. *Agronomy, 11*, 1-22.
34. Razali, N. M., & Wah, Y. B. (2011). Power comparisons of Shapiro-Wilk, Kolmogorov-Smirnov, Lilliefors and Anderson-Darling tests. *Journal of Statistical Modeling and Analytics, 2*(1), 21-33.
35. Rico, C. M., et al. (2011). Interaction of nanoparticles with edible plants and their possible implications in agriculture. *Journal of Agricultural and Food Chemistry, 59*(8), 3485-3498. https://doi.org/10.1021/jf104517j
36. Sangwan, P., et al. (2019). Molybdenum nutrition improves nitrogen metabolism and productivity in wheat under field conditions. *Journal of Plant Nutrition, 42*(18), 2345-2358. https://doi.org/10.1080/01904167.2019.1655036
37. Shapiro, S. S., & Wilk, M. B. (1965). An analysis of variance test for normality (complete samples). *Biometrika, 52*(3-4), 591-611. https://doi.org/10.1093/biomet/52.3-4.591
38. Socrates, G. (2004). *Infrared and Raman characteristic group frequencies: Tables and charts* (3rd ed.). John Wiley & Sons.
39. Tejada-Jiménez, M., et al. (2013). Molybdenum metabolism in plants. *Metallomics, 5*, 1191-1203.
40. Tripathi, D. K., Singh, S., Singh, V. P., et al. (2017). An overview on manufactured nanoparticles in plants: Uptake, translocation, accumulation and phytotoxicity. *Plant Physiology and Biochemistry, 110*, 2-12. https://doi.org/10.1016/j.plaphy.2016.07.030
41. Tukey, J. W. (1949). Comparing individual means in the analysis of variance. *Biometrics, 5*(2), 99-114.
42. von Uexküll, H. R., & Mutert, E. (1995). Global extent, development and economic impact of acid soils. *Plant and Soil, 171*, 1-15.

43. Wang, Y., et al. (2002). Effects of soil acidification on micronutrient availability. *Soil Biology and Biochemistry, 34*, 1043-1050.
44. Zhang, H., et al. (2012). Nitrogen form influences nitrate reductase activity and plant growth. *Plant Physiology and Biochemistry, 58*, 117-123.
45. Zhang, H., Wang, R., Chen, Z., Pu, J., Wang, J., Zhang, H., & Yang, Y. (2022). Nanoscale molybdenum oxide improves plant growth and increases nitrate utilisation in rice (Oryza sativa L.). *Food and Energy Security*, *11*(2). https://doi.org/10.1002/fes3.383